The Protective Role of Nrf2 in Streptozotocin-Induced Diabetic Nephropathy

Tao Jiang,[1,2] Zheping Huang,[1] Yifeng Lin,[2] Zhigang Zhang,[2] Deyu Fang,[3] and Donna D. Zhang[1]

OBJECTIVE—Diabetic nephropathy is one of the major causes of renal failure, which is accompanied by the production of reactive oxygen species (ROS). Nrf2 is the primary transcription factor that controls the antioxidant response essential for maintaining cellular redox homeostasis. Here, we report our findings demonstrating a protective role of Nrf2 against diabetic nephropathy.

RESEARCH DESIGN AND METHODS—We explore the protective role of Nrf2 against diabetic nephropathy using human kidney biopsy tissues from diabetic nephropathy patients, a streptozotocin-induced diabetic nephropathy model in $Nrf2^{-/-}$ mice, and cultured human mesangial cells.

RESULTS—The glomeruli of human diabetic nephropathy patients were under oxidative stress and had elevated Nrf2 levels. In the animal study, Nrf2 was demonstrated to be crucial in ameliorating streptozotocin-induced renal damage. This is evident by $Nrf2^{-/-}$ mice having higher ROS production and suffering from greater oxidative DNA damage and renal injury compared with $Nrf2^{+/+}$ mice. Mechanistic studies in both in vivo and in vitro systems showed that the Nrf2-mediated protection against diabetic nephropathy is, at least, partially through inhibition of transforming growth factor-β1 (TGF-β1) and reduction of extracellular matrix production. In human renal mesangial cells, high glucose induced ROS production and activated expression of Nrf2 and its downstream genes. Furthermore, activation or overexpression of Nrf2 inhibited the promoter activity of TGF-β1 in a dose-dependent manner, whereas knockdown of Nrf2 by siRNA enhanced TGF-β1 transcription and fibronectin production.

CONCLUSIONS—This work clearly indicates a protective role of Nrf2 in diabetic nephropathy, suggesting that dietary or therapeutic activation of Nrf2 could be used as a strategy to prevent or slow down the progression of diabetic nephropathy.
***Diabetes* 59:850–860, 2010**

Among the various types of diabetes complications, diabetic nephropathy is the most common renal complication and the leading cause of end-stage renal disease. The prevalence of diabetes is high in the U.S., Japan, and most industrialized European countries (1). As a chronic disease, diabetic nephropathy is characterized by sequential pathological changes, including renal hypertrophy and basement membrane thickening in the early stage and extracellular matrix (ECM) accumulation, glomerulosclerosis, and interstitial fibrosis in the late stage, which eventually results in the loss of renal function (2,3). Although the pathogenesis of diabetic nephropathy is complex and remains unclear, hyperglycemia is the primary factor that underlies the initiation of diabetic nephropathy (4). It has been demonstrated in several in vitro studies that high glucose–induced renal damage is associated with excessive production of reactive oxygen species (ROS) under hyperglycemic conditions (4–6). In support of this notion, many renal cell types including mesangial cells, endothelial cells, and tubular epithelial cells were found to produce high levels of ROS under hyperglycemic conditions (7–10).

Nrf2 is one of the most important cellular defense mechanisms to cope with oxidative stress (11,12). It regulates intracellular antioxidants, phase II detoxifying enzymes, and many other proteins that detoxify xenobiotics and neutralize ROS to promote cell survival and maintain cellular redox homeostasis (13). NAD(P)H quinone oxidoreductase (NQO1), glutathione S-transferase (GST), heme oxygenase-1 (HO-1), and γ-glutamylcysteine synthetase (γGCS) are among the well-studied Nrf2 target genes that are upregulated through the antioxidant response element regulatory element in response to oxidative stress (14,15). The essential role of Nrf2 in combating oxidative stress induced by a broad spectrum of insults has been clearly demonstrated by the findings demonstrating the increased sensitivity of $Nrf2^{-/-}$ mice to a variety of insults (14). Recently, the essential role of Nrf2 in protecting against diabetic vascular diseases has emerged. Activation of Nrf2 by sulforaphane suppressed hyperglycemia-induced ROS and metabolic dysfunction in human microvascular endothelial cells (16). Using primary cardiomyocytes isolated from $Nrf2^{+/+}$ and $Nrf2^{-/-}$ mice, He et al. (17) demonstrated that Nrf2 conferred protection against high glucose–induced oxidative damage. In another study, Yoh et al. (18) reported a beneficial role of Nrf2 against diabetes using a streptozotocin (STZ)-induced diabetes model. In their study, higher urinary nitric oxide metabolites, higher levels of ROS, and a greater degree of nitrosative DNA damage were detected in STZ-treated $Nrf2^{-/-}$ mice than in STZ-treated $Nrf2^{+/+}$ mice (18).

During the later stages of diabetic nephropathy, transforming growth factor-β1 (TGF-β1) overexpression, ECM deposition, and loss of glomerular architecture define glomerulosclerosis (10). Mounting evidence suggests a role of TGF-β1 in the progression of diabetic nephropathy and glomerulosclerosis by controlling production of many ECM proteins (19–24). For instance, an anti–TGF-β1 antibody was reported to be useful in inhibiting glomerulonephritis by blocking ECM production in a mesangial proliferative glomerulonephritis model (25). Interestingly,

From the [1]Department of Pharmacology and Toxicology, University of Arizona, Tucson, Arizona; the [2]Department of Pathology, Fudan University, Shanghai Medical College, Shanghai, China; and the [3]Department of Pathology, Northwestern University, School of Medicine, Chicago, Illinois.
Corresponding author: Donna D. Zhang, dzhang@pharmacy.arizona.edu.
Received 10 September 2009 and accepted 7 January 2010. Published ahead of print at http://diabetes.diabetesjournals.org on 26 January 2010. DOI: 10.2337/db09-1342.

a recent report indicated the interplay between the TGF-β1 and Nrf2 pathways. Activation of the TGF-β1 pathway was reported to inhibit Nrf2-dependent expression of the γ-glutamylcysteine synthetase catalytic subunit, resulting in elevated ROS levels. This in turn further activated the TGF-β1 pathway, leading to excessive production of ECM (26). On the other hand, activation of Nrf2 is able to inhibit the function of TGF-β1 in a liver fibrosis mouse model (27). Thus, it is conceivable that activation of the Nrf2-mediated antioxidant response is beneficial in preventing or slowing down the progression of diabetic nephropathy by reducing ROS and TGF-β1–mediated ECM production. In this article, we show that kidneys from diabetic nephropathy patients are under oxidative stress. Consistent with the notion that Nrf2 is beneficial in suppressing the progression of diabetic nephropathy, we observed that $Nrf2^{-/-}$ mice suffered greater STZ-induced renal damage. Furthermore, a negative role of Nrf2 in controlling the promoter activity of TGF-β1 and ECM production was demonstrated in human mesangial cells (HRMCs).

RESERCH DESIGN AND METHODS

Patients and renal histology. The diabetic nephropathy kidney tissues were obtained from eight patients with proteinuria that underwent a renal biopsy for diagnosis of diabetic nephropathy at the Department of Pathology, Shanghai Medical College, Fudan University, China, in 2007 or 2008. All cases were diagnosed by two individual pathologists in a double-blind manner. Eight patients who underwent kidney transplants were biopsied 1 year later to ensure normal function of their transplanted kidney. These biopsies were then used as the normal kidney specimens in our study. Permission to use the fixed tissue sections for research purposes was obtained and approved by the Ethics Committee from Shanghai Medical College, Fudan University, China, and a written consent form was obtained from all patients. The paraffin sections were stained with hematoxylin and eosin (H&E), Congo red, periodic acid Schiff (PAS), and immunofluorescence depositions for diagnosis of diabetic nephropathy.

Animals and treatments. $Nrf2^{-/-}$ mice in C57BL/6 background were gifts from Dr. Jeff Chan (University of California, Irvine) (28). $Nrf2^{+/+}$ and $Nrf2^{-/-}$ mice (eight mice per group), at 8 weeks of age, were intraperitoneally injected with STZ (50 mg/kg, pH 4.5) dissolved in sodium citrate or injected with vehicle (sodium citrate only) for 5 consecutive days. At 16 weeks post-injection, the mice were killed and the kidneys were isolated.

Blood glucose and urine albumin-to-creatinine ratio measurement. Blood glucose levels from the tail-vein were measured by the OneTouch Blood Glucose Monitoring System (LifeScan, Milpitas, CA) at 3, 5, 8, 12, and 16 weeks post-injection. The mice fasted for 4 h before blood glucose measurement. Freshly voided spot urine samples were collected at 1, 8, and 16 weeks post-injection. Urine albumin and creatinine levels were measured by ELISA kits (albumin: Bethyl Laboratories, Houston, TX; creatinine: Exocell, Philadelphia, PA). The urine albumin-to-creatinine ratio (UACR) was expressed as the ratio of albumin to creatinine.

Mouse renal histology and detection of oxidative DNA damage. Both kidneys from each mouse were isolated and cut into two halves. The tissue was cut into 4-μm sections and stained with H&E, PAS, and Masson's trichrome. For PAS-stained tissue sections, a five-grade method was used to evaluate the sclerosis in glomeruli as described (29). The protocol for detection of *8*-dihydro-2′-deoxyguanosine (8-Oxo-dG) requires an additional step: the deparaffinized sections were incubated with proteinase K (10 μg/ml) for 30 min at 37°C and RNase A (100 μg/ml) for 1 h at 37°C and then exposed to 2 N HCl for 5 min at room temperature, followed by the immunohistochemical analysis. Urinary 8-Oxo-dG was measured using liquid chromatography–mass spectrometry/mass spectrometry.

Immunohistochemical analysis and antibodies. Kidney tissues were fixed in 4% buffered paraformaldehyde and embedded in paraffin. The deparaffinized sections were boiled in sodium citrate buffer. The primary antibody was used in a dilution of 1:100 for 1 h at 37°C and 4°C overnight. For human tissues, an anti-Nrf2 antibody from Abcam (Cambridge, MA) was used. For mouse tissues, an anti-Nrf2 polyclonal antibody was used (Santa Cruz Biotechnology, Santa Cruz, CA). Antibodies against 8-Oxo-7, 8-Oxo-dG (Gaithersburg, MD), and fibronectin (FN) (Calbiochem, San Diego, CA) were purchased from commercial sources. NQO1, aldose reductase, γGCS, and glyceraldehyde-3-phosphate dehydrogenase (GAPDH) antibodies were all purchased from Santa Cruz.

TABLE 1
Primers and probes used for quantitative RT-PCR

	Probe	Primer nucleotide sequences
mNrf2	#56	Forward: ttttccattcccgaattacagt
		Reverse: aggagatcgatgagtaaaaatggt
mNQ01	#50	Forward: agggttcggtattacgatcc
		Reverse: agtacaatcagggctcttctcg
mGST	#75	Forward: tctgacccctttccctctg
		Reverse: ctgccaggctgtaggaacct
mTGF-β1	#56	Forward: tcagacattcgggaagcagt
		Reverse: acgccaggaattgttgctat
mFibronectin	#50	Forward: cacggaggccaccattact
		Reverse: cttcagggcaatgacgtagat
mcollagen IV α	#56	Forward: ttaaaggactccagggaccac
		Reverse: cccactgagcctgtcacac
mβ-actin	#56	Forward: aaggccaaccgtgaaaagat
		Reverse: gtggtacgaccagaggcatac
hNrf2	#70	Forward: acacggtccacagctcatc
		Reverse: tgtcaatcaaatccatgtcctg
hNQO1	#87	Forward: atgtatgacaaaggacccttcc
		Reverse: tcccttgcagagagtacatgg
nHO-1	#25	Forward: aactttcagaagggccaggt
		Reverse: ctgggctctccttcttgc
hGST	#56	Forward: tccctcatctacaccaactatgag
		Reverse: ggtcttgcctccctggtt
hGAPDH	#25	Forward: ctgacttcaacagcgacacc
		Reverse: tgctgtagccaaattcgttgt

qRT-PCR and immunoblot assay. Total RNA from kidney tissues or HRMCs was extracted using Trizol solution. Equal amounts of RNA (2 μg) was reverse-transcripted into cDNA using the Transcriptor First Strand cDNA Synthesis Kit (Roche, IN). Taqman probes and primers used in this study are listed in Table 1. For the bar graph in Fig. 5*A*, the data represent the average of eight mice in the same group, each with duplicated samples for qRT-PCR. The data were expressed as relative mRNA levels normalized to β-actin, and the value from the $Nrf2^{+/+}$ control was set as 1. For the in vitro study with HRMCs, the experiments were repeated three times with duplicate samples. For immunoblot analysis, the frozen kidneys were homogenized in lysis buffer (0.1 mol/l Tris buffer [pH 7.4], 0.1 mmol/l EDTA) in the presence of 1 mmol/l dithiothreitol, 1 mmol/l phenylmethylsulfonyl fluoride, and a protease inhibitor cocktail (Roche, IN). Protein concentration was determined using the Bio-Rad DC Protein Assay (Bio-Rad, CA). Protein (300 μg) was loaded into each well and subjected to immunoblot analysis. Each lane in Fig. 5*C* contained proteins extracted from the kidney of individual mice.

Cell culture, ROS detection, siRNA transfection, and luciferase reporter gene assay. HRMCs were purchased from ScienCell Research Laboratories (Carlsbad, CA) and maintained in RPMI-1640 supplemented with 2% FBS and mesangial cell growth supplement (ScienCell Research Laboratories). After growth arrested in 0.5% FBS for 24 h, cells were cultured in either low (1 g/l) or high (5.4 g/l) glucose Dulbecco's modified Eagle's medium (DMEM) for an additional 24 h before harvest. For ROS measurement, cells were then incubated for 30 min with dichlorofluorescein (5 μg/ml) (Sigma, St. Louis, MO), and the fluorescence intensity was measured by flow cytometry. Nrf2-siRNA and HiPerfect transfection reagent were purchased from Qiagen (Valencia, CA), and transfection of Nrf2-siRNA was performed according to the manufacturer's instruction. For luciferase reporter gene assay, HRMCs were transfected with plasmids for TGF-β1–promoter-firefly luciferase and renilla luciferase, along with different amounts of an expression vector for Nrf2, and then firefly and renilla luciferase activities were measured using a dual-luciferase reporter gene assay system (Promega, Madison, WI).

Statistical analysis. Results were expressed as means ± SD. Statistical tests were performed using SPSS 10.0. Unpaired Student's *t* tests were used to compare the means of two groups. One-way ANOVA was applied to compare the means of three or more groups. The Wilcoxon (Gehan) statistical test was used to analyze survival rate. $P < 0.05$ was considered to be significant.

RESULTS

The glomeruli of human diabetic nephropathy patients were under oxidative stress and underwent significant pathological changes. In total, tissues from eight normal and eight diabetic nephropathy kidneys were

TABLE 2
Selected clinical characteristics of patients in the study group

	Control	Diabetic nephropathy patients with proteinuria
n	8	8
Sex (M/F)	6/2	7/1
Age	59 ± 8	47 ± 5
Duration of diabetes	N	13 ± 8
A1C (%)	NA	8.8 ± 0.9
Systolic blood pressure (mmHg)	NA	127 ± 14
Diastolic blood pressure (mmHg)	NA	76 ± 12
BMI (kg/m^2)	NA	26 ± 4.8
Albumin excretion rate (μg/min)	NA	664.2 (233.0–769.1)

Data are means ± SD. N, no diabetic nephropathy. NA, not available.

selected for this study. The selected clinical characteristics of patients are shown in Table 2. Pathological and immunohistochemical analyses were performed (Fig. 1). Compared with normal glomeruli, the glomeruli from diabetic nephropathy patients showed significant morphological changes (Fig. 1, compare *A* and *B*). Two massive K-W nodules were formed inside the glomerulus of diabetic nephropathy patients (Fig. 1*B*, *white arrows*). It has been reported that overproduction of ROS is one of the major factors mediating tissue damage in diabetes (30). Thus, Nrf2 is likely activated in the glomeruli of diabetic nephropathy patients. Next, Nrf2 expression in normal and diabetic nephropathy glomeruli was measured using immunohistochemical analysis. Nrf2 was hardly expressed in normal glomeruli, whereas it was upregulated in diabetic nephropathy glomeruli (Fig. 1, compare *C* and *D*). In addition, cells with high expression of Nrf2 in the nucleus were identified as mesangial cells (Fig. 1*D*, *arrows*). NQO1, a well-studied Nrf2 target gene, was also activated in glomeruli of diabetic nephropathy patients (Fig. 1, compare *E* and *F*), indicating the activation of the Nrf2-mediated antioxidant response. Next, oxidative DNA damage was measured using immunohistochemical analysis with an anti–8-Oxo-dG antibody. Nuclear staining was detected in some cells of the glomeruli from diabetic nephropathy patients, indicting that the diabetic nephropathy kidney is under oxidative damage (Fig. 1, compare *G* and *H*). However, the number of nuclear stained cells was low in diabetic nephropathy patients because of the massive glycogen deposition inside the glomeruli (Fig. 1*H*). Together, these results demonstrated that the glomeruli of diabetic nephropathy patients are under severe oxidative stress and the Nrf2-mediated antioxidant response is activated.

Nrf2$^{-/-}$ mice suffered greater renal damage induced by STZ compared with Nrf2$^{+/+}$ mice. During the course of 16 weeks, some mice in both STZ-treated Nrf2$^{+/+}$ and Nrf2$^{-/-}$ groups died, but the survival rate between the two groups did not show any statistical difference (Fig. 2*A*, $P = 0.9477$). Blood glucose levels, monitored at 3, 5, 8, 12, and 16 weeks post-injection, were significantly increased in both Nrf2$^{+/+}$ and Nrf2$^{-/-}$ mice after STZ treatment, although no difference in glucose levels was observed between the two genotype groups (Fig. 2*B*, $*P < 0.05$).

At 16 weeks post-injection, mice in the STZ-treated groups had a decrease in their body weight, whereas the untreated groups gained weight (Fig. 2*C*, $*P < 0.05$). Interestingly, Nrf2$^{-/-}$ mice lost more body weight than Nrf2$^{+/+}$ mice when treated with STZ (Fig. 2*C*, $\#P < 0.05$). Next, the ratio of kidney to body weight, which indicates the enlargement of the kidney, was calculated. The ratio was significantly increased in the STZ-treated groups (Fig. 2*D*, $*P < 0.05$). However, there was no difference in the ratio of kidney to body weight between the two genotypes, even in the treated groups, which may be due to the greater decrease in body weight of the Nrf2$^{-/-}$ mice (Fig. 2*D*). As an index of renal function, UACR was measured at 0, 8, and 16 weeks after STZ injection. STZ markedly enhanced UACR at both 8 and 16 weeks post-injection (Fig. 2*E*, $*P < 0.05$). Although no difference was observed between Nrf2$^{+/+}$ and Nrf2$^{-/-}$ mice at 8 weeks post-injection, the Nrf2$^{-/-}$ mice showed a significantly higher UACR than Nrf2$^{+/+}$ mice at 16 weeks post-injection (Fig. 2*E*, $\#P < 0.05$). All these results indicate that Nrf2$^{-/-}$ mice suffered greater renal damage, implicating the essential role of Nrf2 in protecting against STZ-induced diabetic nephropathy.

Higher levels of oxidative stress and oxidative damage occurred in the glomeruli of Nrf2$^{-/-}$ mice than in Nrf2$^{+/+}$ mice in response to STZ. Next, STZ-induced oxidative stress were measured by Nrf2 activation and oxidative DNA damage. Nrf2$^{-/-}$ mice did not have any detectable levels of Nrf2 in their glomeruli, confirming the complete deletion of Nrf2 (Fig. 3*A*, *c* and *d*). Nrf2 expression was greatly enhanced in the glomeruli of the STZ-treated Nrf2$^{+/+}$ group and Nrf2 nuclear staining was observed (Fig. 3*A*, compare *a* and *b*, and the *insert* of *b*). Activation of Nrf2 was confirmed by upregulation of NQO1 in response to STZ treatment in Nrf2$^{+/+}$ mice, but not in Nrf2$^{-/-}$ mice (Fig. 3*A*, *i–l*). To test the role of Nrf2 in ameliorating oxidative damage under the diabetic nephropathy condition, oxidative DNA damage was compared in the glomeruli of Nrf2$^{+/+}$ and Nrf2$^{-/-}$ mice using immunohistochemical analysis with an anti–8-Oxo-dG antibody. The results reveal that the STZ-treated Nrf2$^{-/-}$ mice had a greater degree of oxidative damage than the STZ-treated Nrf2$^{+/+}$ mice (Fig. 3*A*, compare *f* and *h*). Intriguingly, Nrf2$^{-/-}$ mice displayed higher levels of oxidative damage even in the untreated condition (Fig. 3*A*, compare *e* and *g*), indicating that the basal level of Nrf2 is essential in protecting against DNA damage induced by intrinsic sources of ROS. Consistent with these results, higher levels of basal and STZ-induced oxidative DNA damage in Nrf2$^{-/-}$ mice were confirmed by measuring the urinary level of 8-Oxo-dG (Fig. 3*B*). These results clearly demonstrate that Nrf2$^{-/-}$ mice had higher production of ROS in response to STZ challenge and were more vulnerable to ROS-induced damage due to loss of Nrf2.

Nrf2$^{-/-}$ mice had more severe glomerular injury than Nrf2$^{+/+}$ mice. Kidneys were isolated and processed for pathological analysis using H&E, PAS, and Masson's trichrome staining. Glomerular lesions were detected in both Nrf2$^{+/+}$ and Nrf2$^{-/-}$ mice after STZ injection in H&E-stained tissue sections (Fig. 4*A*, compare *a* and *b*, and *c* and *d*; K-W nodules are labeled with arrows in *b* and *d*). Next, glycogen deposition was measured by PAS staining (Fig. 4*A*, *e–h*). The severity of glomerulosclerosis was scored using a semiquantitative method, and the result is shown in Fig. 4*B*. STZ significantly induced glomerulosclerosis in both genotype groups (Fig. 4*A*, compare *e* and *f*, and *g* and *h*; Fig. 4*B*, $*P < 0.05$). Moreover, Nrf2$^{-/-}$ mice showed a higher score than

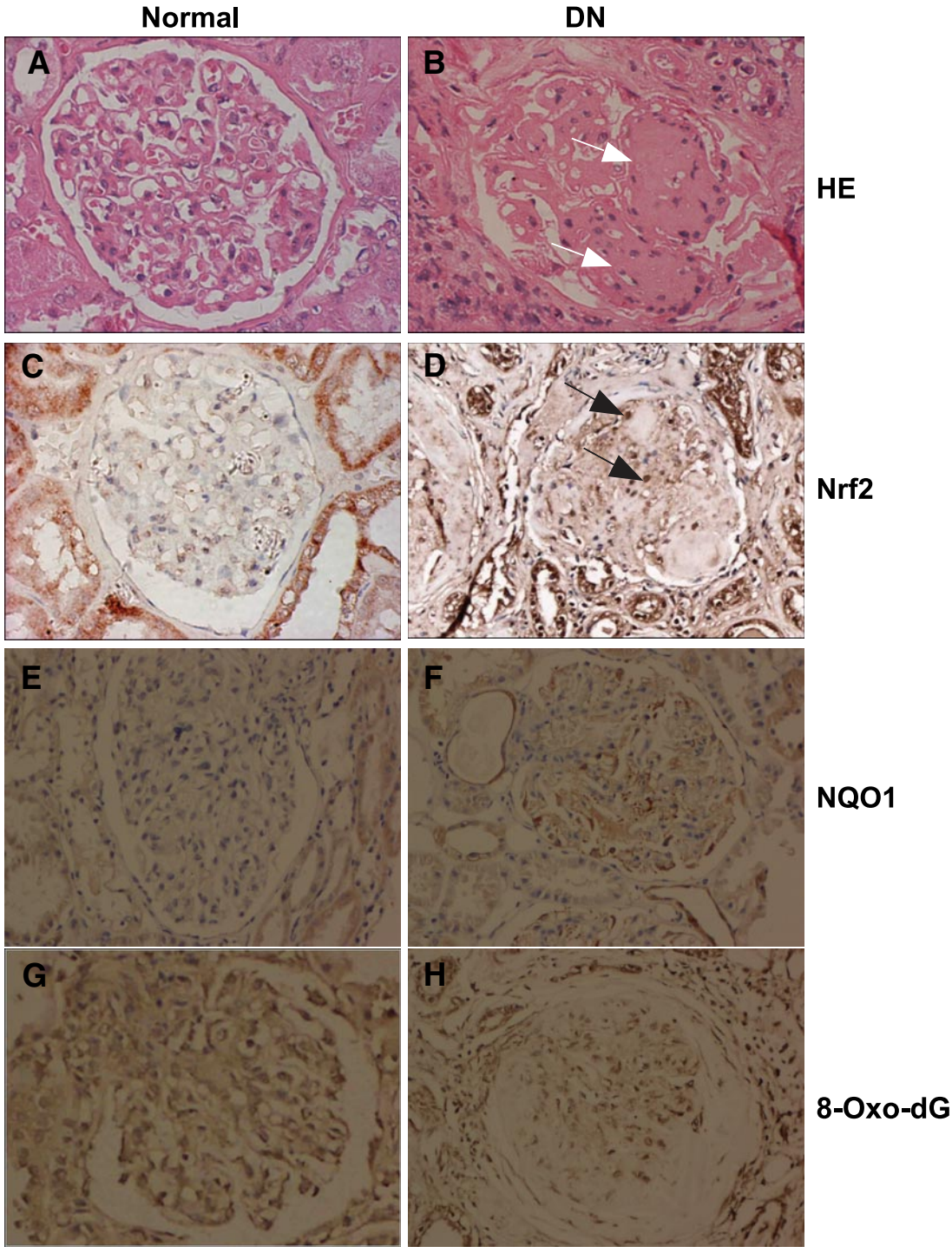

FIG. 1. Significant pathological changes and activation of Nrf2 pathway in the glomeruli of human diabetic nephropathy patients. Renal biopsy samples were fixed and cut into 2-μm sections; the sections were subjected to H&E staining (*A* and *B*) and immunohistochemical analysis with anti-Nrf2 (*C* and *D*), anti-NQO1 (*E* and *F*), and anti–8-Oxo-dG (*G* and *H*) antibodies. The images shown are representative of eight normal kidney tissue patients (*A*, *C*, *E*, and *G*) and eight kidney tissues from diabetic nephropathy patients (*B*, *D*, *F*, and *H*). Magnification is 400×. White and black arrows (*B* and *D*) indicate K-W nodules and the Nrf2-positive nuclei, respectively. (A high-quality color representation of this figure is available in the online issue.)

$Nrf2^{+/+}$ mice in response to STZ treatment (Fig. 4*A*, compare *f* and *h*; Fig. 4*B*, #$P < 0.05$). In addition, K-W nodules were also observed in PAS-stained tissues in the STZ-treated groups (Fig. 4*A*, compare *e* and *f*, and *g* and *h*, black arrows in *f* and *h*). ECM deposition in glomeruli is a hallmark of many renal diseases including diabetic nephropathy (31,32), Therefore, collagens and FN, the major components of ECM, were measured using Masson's trichrome staining method and immunohistochemical analysis with an anti-FN antibody, respectively. Collagen deposition was observed inside the glomeruli of the STZ-treated $Nrf2^{-/-}$ mice, but not in STZ-treated $Nrf2^{+/+}$ mice (Fig. 4*A*, compare *j* and *l*). Slight collagen deposition in the untreated $Nrf2^{-/-}$ mice was also observed (Fig. 4*A*, *k*). In response to STZ treatment, expression of FN was increased in both genotype groups (Fig. 3*A*, compare *m* and

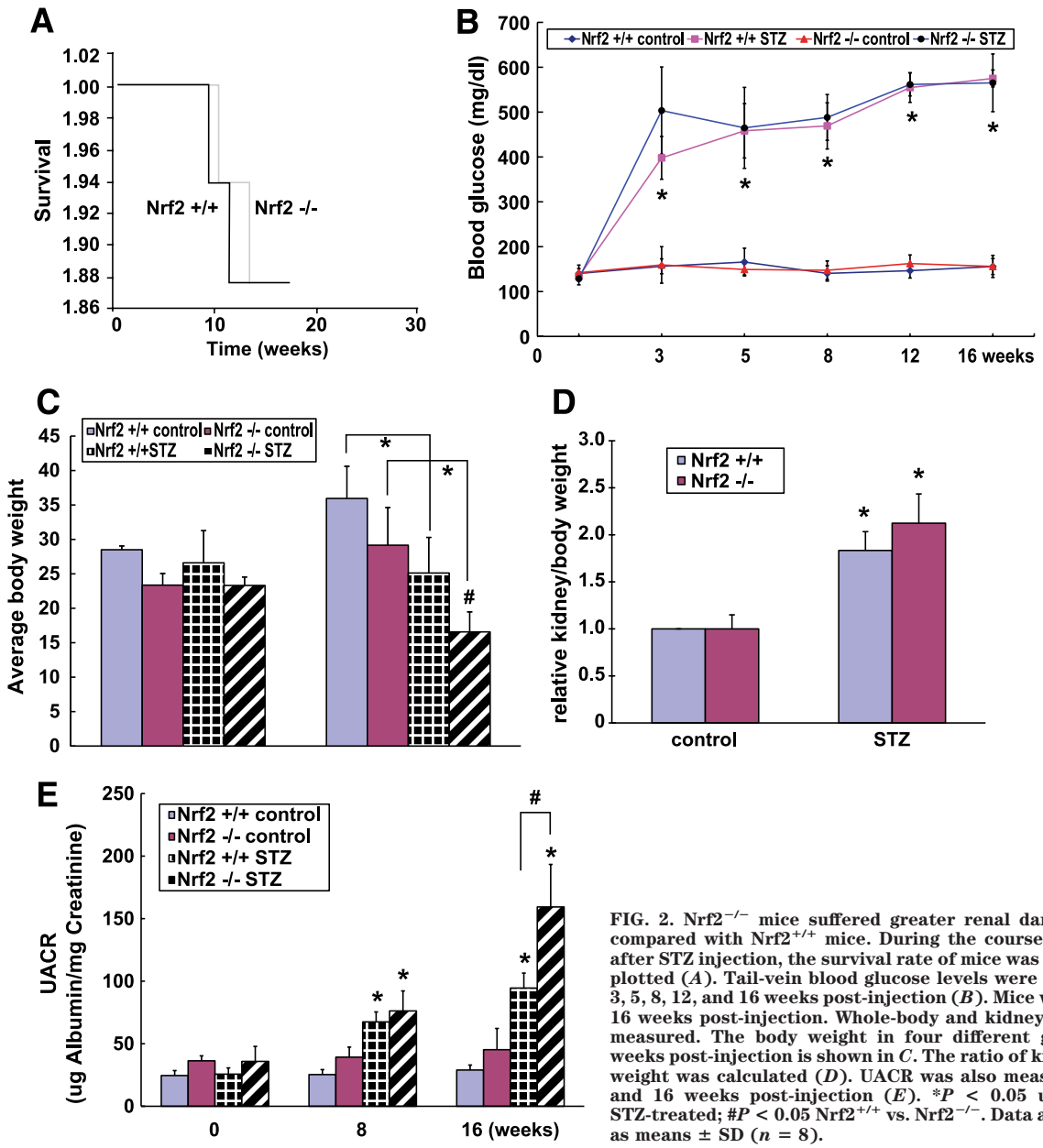

FIG. 2. Nrf2$^{-/-}$ mice suffered greater renal damage by STZ compared with Nrf2$^{+/+}$ mice. During the course of 16 weeks after STZ injection, the survival rate of mice was recorded and plotted (*A*). Tail-vein blood glucose levels were monitored at 3, 5, 8, 12, and 16 weeks post-injection (*B*). Mice were killed at 16 weeks post-injection. Whole-body and kidney weight were measured. The body weight in four different groups at 16 weeks post-injection is shown in *C*. The ratio of kidney to body weight was calculated (*D*). UACR was also measured at 0, 8, and 16 weeks post-injection (*E*). *$P < 0.05$ untreated vs. STZ-treated; #$P < 0.05$ Nrf2$^{+/+}$ vs. Nrf2$^{-/-}$. Data are expressed as means ± SD ($n = 8$).

n, and *o* and *p*). Consistent with the observed oxidative damage in untreated Nrf2$^{-/-}$ mice (Fig. 3*A*, *g*), the basal level of FN expression in Nrf2$^{-/-}$ was also higher than that in Nrf2$^{+/+}$ mice (Fig. 4*A*, compare *m* and *o*). Collectively, these results demonstrate that Nrf2 is essential in protecting against both basal and STZ-induced glomerular injury.

Nrf2$^{-/-}$ mice had higher TGF-β1 transcription and FN expression. Next, the molecular mechanism by which Nrf2 protects against STZ-induced glomerular injury was explored. First, activation of the Nrf2 pathway by STZ-induced ROS was tested. Data shown in Fig. 5*A* represent the average reading of eight mice in each group. As expected, there was no Nrf2 mRNA detected in Nrf2$^{-/-}$ mice (Fig. 5*A*, *Nrf2 panel* #$P < 0.05$). In addition, STZ treatment did not induce Nrf2 mRNA expression in Nrf2$^{+/+}$ mice (Fig. 5*A*, *Nrf2 panel*), which is consistent with the previous findings that upregulation of Nrf2 is primarily regulated at the level of Nrf2 protein stability. However, the downstream genes of Nrf2, NQO1, and GST were transcriptionally activated in response to STZ in Nrf2$^{+/+}$ mice and only slightly in Nrf2$^{-/-}$ mice (Fig. 5, *NQO1 and GST panels*, *$P < 0.05$), indicating the activation of the Nrf2-mediated antioxidant response. Intriguingly, although both basal and STZ-induced levels of NQO1 in Nrf2$^{-/-}$ mice were lower than that in Nrf2$^{+/+}$ mice, the basal level of GST was similar between these two genotype groups (Fig. 5*A*, *NQO1 panel*, #$P < 0.05$, and *GST panel*).

Next, mRNA expression of TGF-β1, FN, and collagen IV were measured. As shown in Fig. 5*B*, the basal level of TGF-β1 in Nrf2$^{-/-}$ mice is higher than Nrf2$^{+/+}$ mice (Fig. 5*B*, *TGF-β1 panel*, #$P < 0.05$). STZ treatment induced transcription of TGF-β1 in both Nrf2$^{+/+}$ and Nrf2$^{-/-}$ mice, and the highest transcription was observed in the STZ-treated Nrf2$^{-/-}$ mice (Fig. 5*B*, *TGF-β1 panel*, *$P < 0.05$, #$P < 0.05$). In agreement with the notion that TGF-β1 positively regulates expression of FN, the mRNA expression pattern of FN is similar to that of TGF-β1 (Fig. 5*B*, *FN panel*, *$P < 0.05$, #$P < 0.05$), demonstrating that FN was overexpressed, especially in the STZ-treated Nrf2$^{-/-}$ mice.

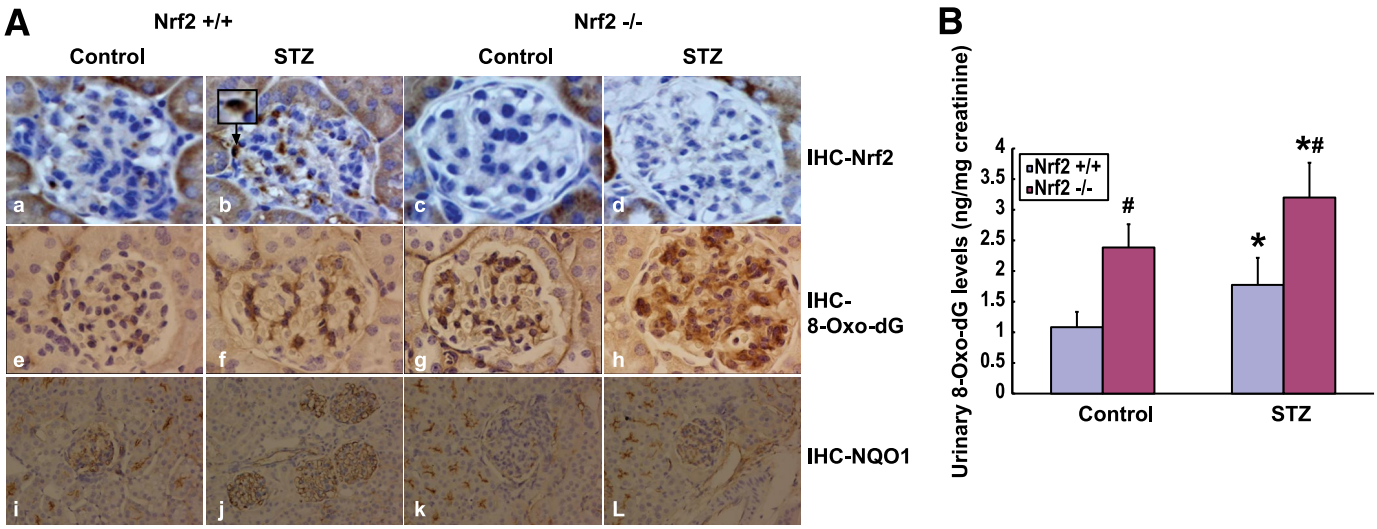

FIG. 3. Higher levels of oxidative stress and oxidative damage occurred in the glomeruli of Nrf2$^{-/-}$ mice than in Nrf2$^{+/+}$ mice in response to STZ. At 16 weeks post-injection, Nrf2$^{+/+}$ and Nrf2$^{-/-}$ mice were killed and kidneys were isolated. Kidney tissue sections from each mouse were used for immunohistochemical analysis with anti-Nrf2 (*A*, *a–d*), anti–8-Oxo-dG (*A*, *e–h*), and anti-NQO1 (*A*, *i–L*) antibodies. Nuclear staining of Nrf2 is shown in the insert (Fig. *A*, *b*). Each image is a representative of eight kidney tissue sections from eight mice in each group. Urinary 8-Oxo-dG was detected by liquid chromatography–mass spectrometry (*B*). *$P < 0.05$ vs. Nrf2$^{+/+}$ mice; #$P < 0.05$. (A high-quality color representation of this figure is available in the online issue.)

To our surprise, although the basal level of collagen IV mRNA expression in Nrf2$^{-/-}$ mice was higher, compared with Nrf2$^{+/+}$ mice (Fig. 5*B*, *collagen IV panel*, #$P < 0.05$), there was no difference in collagen IV mRNA expression between the control and STZ-treated groups. It is likely that the observed collagen deposition in the glomeruli of the STZ-treated Nrf2$^{-/-}$ mice in the Masson's trichrome stained tissues (Fig. 4, *l*) came from other types of collagen, rather than collagen IV. In another set of experiments, NQO1 and FN were chosen as representative Nrf2 and TGF-β1 downstream genes, respectively, and their protein levels were measured by immunoblot analysis. NQO1 was induced by STZ treatment in Nrf2$^{+/+}$ mice, while there was no detectable level of NQO1 in Nrf2$^{-/-}$ mice (Fig. 5*C*, *NQO1 panel*). Quantification data showed nearly fourfold induction of NQO1 in response to STZ in Nrf2$^{+/+}$ mice (Fig. 5*C*, *lower left panel*, *$P < 0.05$). The protein level of FN was induced more than three- to

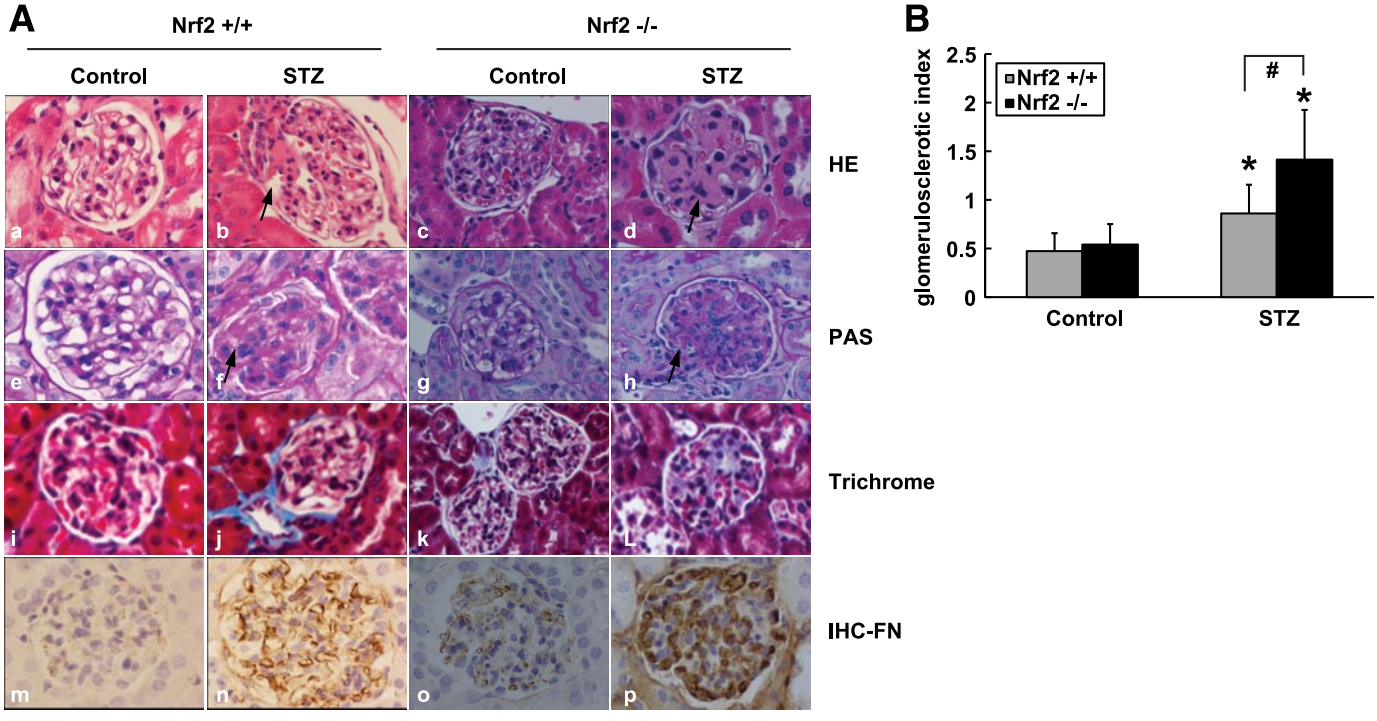

FIG. 4. Nrf2$^{-/-}$ mice had more severe glomerular injury than Nrf2$^{+/+}$ mice. Kidney tissue sections were subject to H&E (Fig. *A*, *a–d*), PAS (*A*, *e–h*), and trichrome staining (*A*, *i–L*), as well as immunohistochemical analysis with an anti-FN antibody (*A*, *m–p*). Each image is a representative of eight kidney tissue sections from eight mice in each group. PAS-stained tissues were used for semiquantitative scoring as described in the RESEARCH DESIGN AND METHODS. Glomerulosclerosis index for four different groups is shown in *B*. In total, 30 glomeruli were scored for each mouse. *$P < 0.05$ untreated vs. STZ-treated; #$P < 0.05$ Nrf2$^{+/+}$ vs. Nrf2$^{-/-}$. Data are expressed as means ± SD ($n = 8$). (A high-quality color representation of this figure is available in the online issue.)

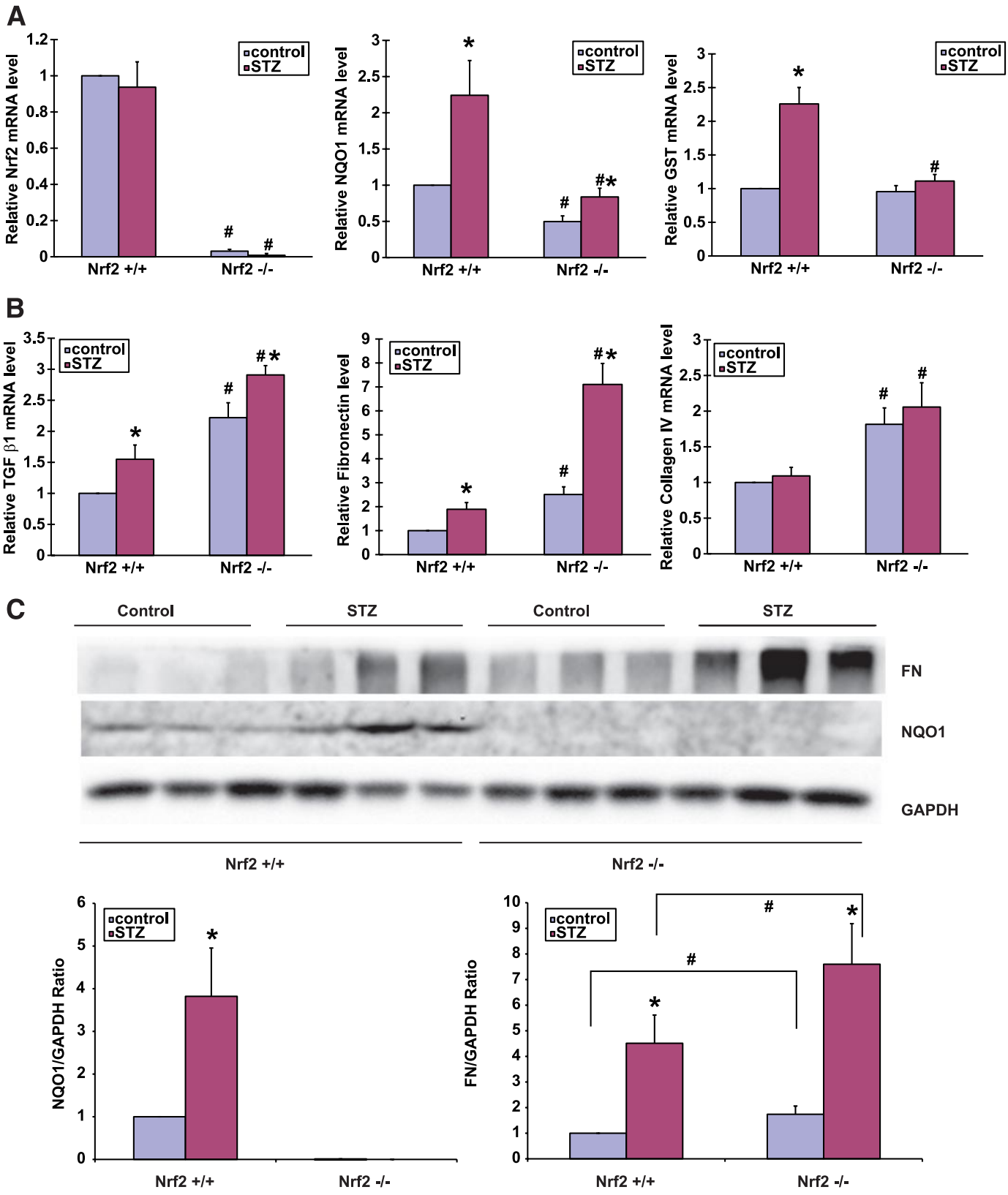

FIG. 5. Nrf2$^{-/-}$ mice had higher TGF-β1 transcription and FN expression. The mRNA level of Nrf2, NQO1, and GST (*A*) and TGF-β1, FN, and collagen IV (*B*) was measured by qRT-PCR. The data presented are relative mRNA level normalized to β-actin mRNA level, and the value from the untreated Nrf2$^{+/+}$ group was set as 1. *$P < 0.05$ untreated vs. STZ-treated; #$P < 0.05$ Nrf2$^{+/+}$ vs. Nrf2$^{-/-}$. Data are expressed as means ± SD ($n = 8$). The protein level of FN, NQO1, and GAPDH was measured by immunoblot analysis (*C*, *upper panel*). Each lane contained total proteins from the kidney of different individual mice. The band intensity was calculated and normalized to GAPDH (*C*, *lower panel*). The value from the untreated Nrf2$^{+/+}$ group was set as 1. *$P < 0.05$ untreated vs. STZ-treated; #$P < 0.05$ Nrf2$^{+/+}$ vs. Nrf2$^{-/-}$. Data are expressed as means ± SD ($n = 3$).

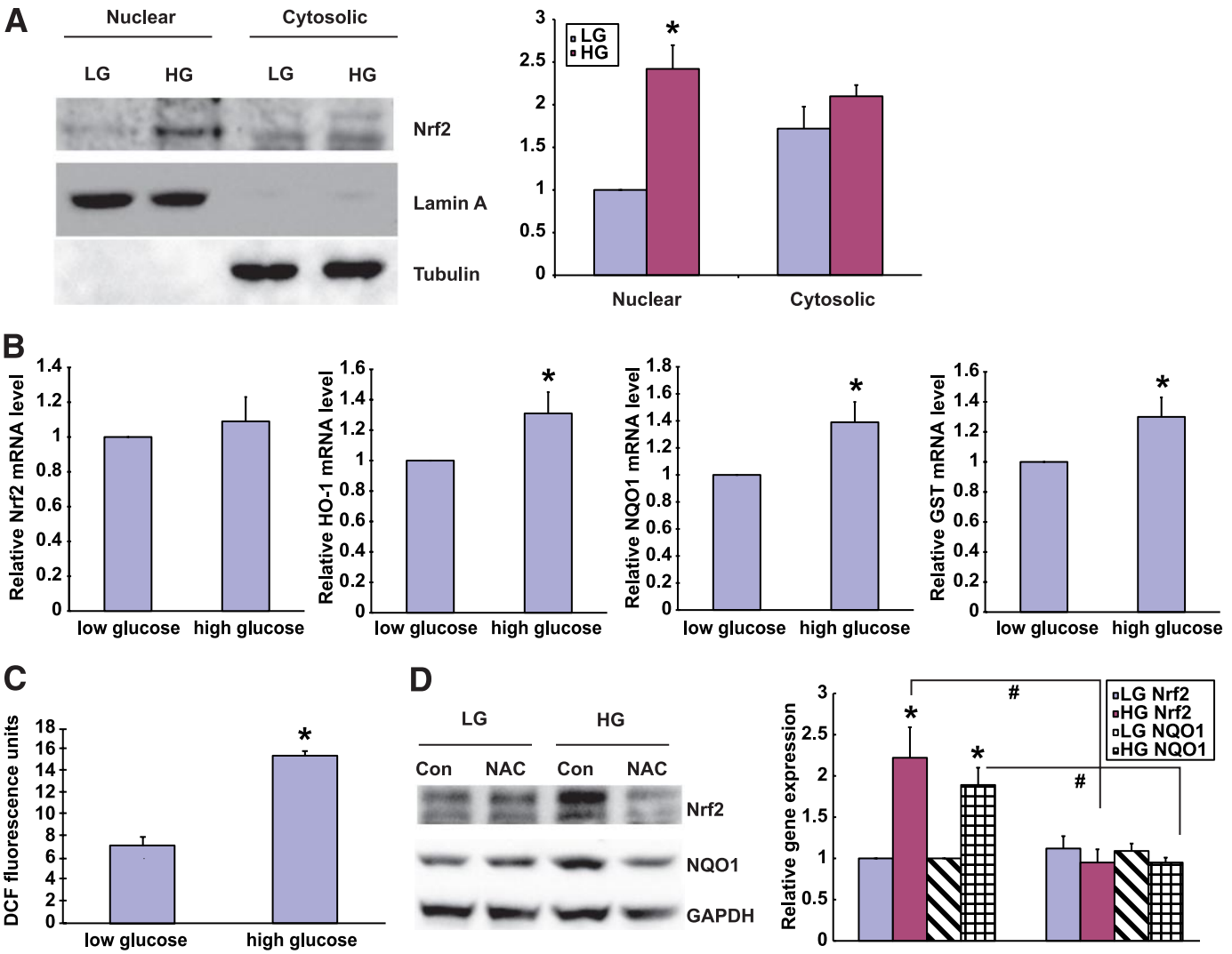

FIG. 6. Nrf2 was activated by high glucose–induced ROS production in HRMCs. Before exposure to low-glucose (LG) (1 g/l) or high-glucose (HG) (5.4 g/l) DMEM, cells were starved for 24 h with low-glucose DMEM containing 0.5% FBS. Cells were then incubated in low- and high-glucose DMEM for an additional 24 h. Nuclear and cytosolic fractions were extracted and subjected to immunoblot analysis using anti-Nrf2, anti-lamin A, and anti-tubulin antibodies (*A*, *left panel*). The intensity of the bands was calculated and quantified (*A*, *right panel*). Total mRNA was extracted and used for qRT-PCR for measurement of the mRNA level of Nrf2, HO-1, NQO1, or GST (*B*). ROS level was also measured in these cells growing in low- or high-glucose medium by dichlorofluorescein (DCF)/flow cytometry analysis described in RESEARCH DESIGN AND METHODS (*C*). HRMCs were incubated with NAC (50 μmol/l) for 24 h. Total cell lysates were subjected to immunoblot analysis using anti-Nrf2, anti-NQO1, and anti-GAPDH antibodies (*D*, *left panel*). The intensity of the bands was quantified (*D*, *right panel*).

fourfold by STZ treatment, both in $Nrf2^{+/+}$ and $Nrf2^{-/-}$ mice (Fig. 5*C*, *FN panel*, and *lower right panel*, $*P < 0.05$). Furthermore, $Nrf2^{-/-}$ mice had both higher basal and STZ-induced levels of FN than $Nrf2^{+/+}$ mice, with the highest FN expression detected in the STZ-treated $Nrf2^{-/-}$ mice (Fig. 5*C*, *FN panel*, and *lower right panel*, $\#P < 0.05$). Taken together, these data demonstrate that STZ is able to activate the Nrf2-mediated antioxidant response, which in turn negatively regulates TGF-β1–mediated ECM production, especially FN.

Nrf2 was activated by high glucose–induced ROS production in HRMCs. To further confirm that the activation of Nrf2 by STZ in vivo is due to high glucose–induced ROS production, in vitro experiments were carried out. Because mesangial cells play a crucial role in the initiation and progression of many renal diseases, including diabetic nephropathy (31,33), HRMCs were used for this in vitro study. An enhanced nuclear protein level of Nrf2 was detected in cells growing under high glucose medium compared with low glucose medium (Fig. 6*A*, $*P < 0.05$). Consistent with this result, high glucose induced the mRNA level of NQO1, HO-1, and GST, without affecting Nrf2 mRNA levels (Fig. 6*B*, $*P < 0.05$), indicating the activation of the Nrf2 pathway. This in vitro study recapitulates the observed Nrf2 activation in STZ-treated $Nrf2^{+/+}$ mice and in human renal tissues from a diabetic nephropathy patient. It is conceivable that high glucose induced Nrf2 activity through ROS production. Thus, ROS levels were measured. Indeed, the cells growing in high glucose medium had substantially higher levels of ROS (Fig. 6*C*, $*P < 0.05$). To further confirm the notion that Nrf2 activation by high glucose is through generation of ROS, *N*-acetylcysteine (NAC), a ROS scavenger, was included in the medium. As shown in Fig. 6*D*, NAC inhibited the activation of high glucose–induced Nrf2 and NQO1 (Fig. 6*D*, $*P < 0.05$, $\#P < 0.05$). Collectively, these results indicate that hyperglycemia is able to activate the Nrf2 pathway through generation of ROS.

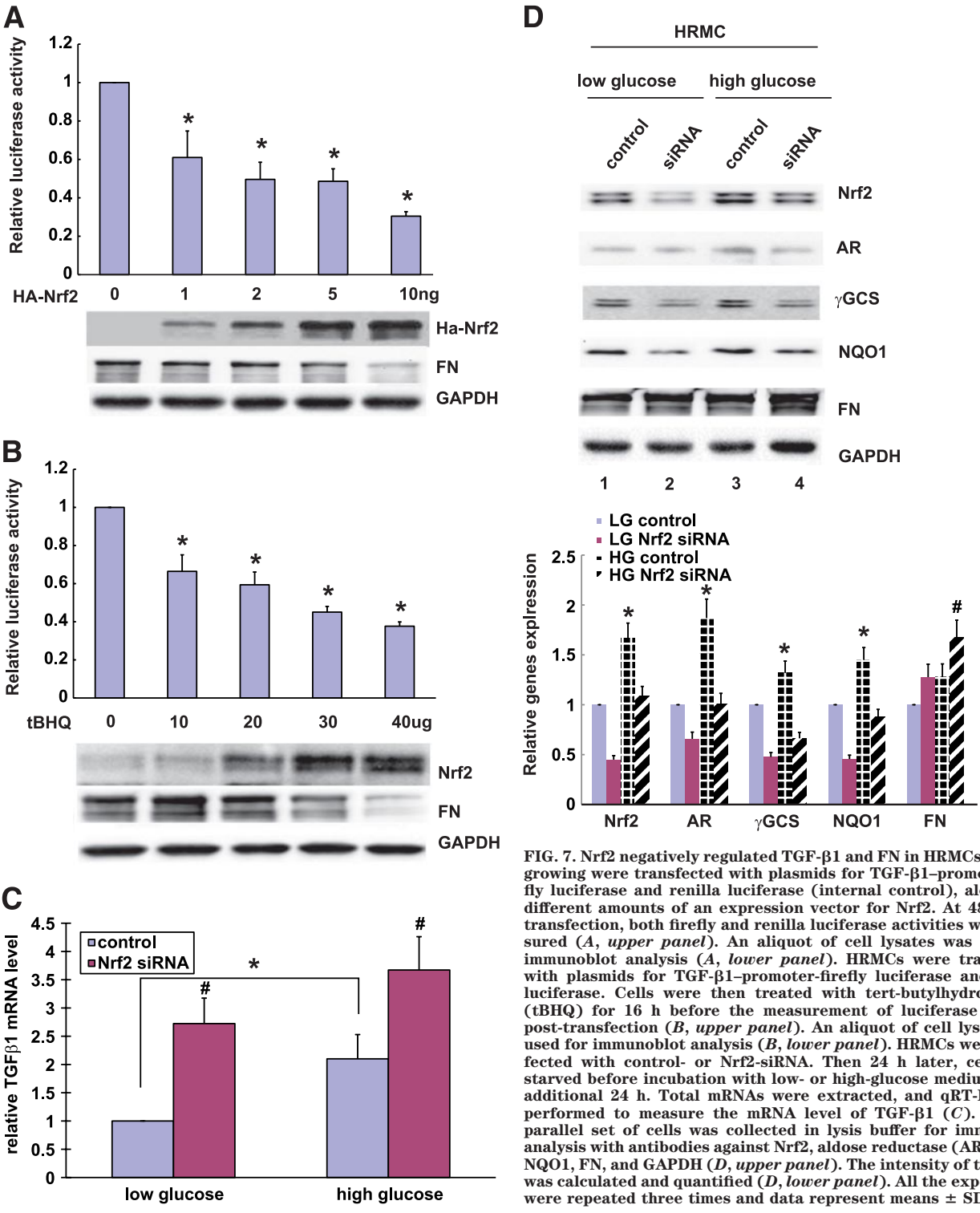

FIG. 7. Nrf2 negatively regulated TGF-β1 and FN in HRMCs. HRMCs growing were transfected with plasmids for TGF-β1–promoter-firefly luciferase and renilla luciferase (internal control), along with different amounts of an expression vector for Nrf2. At 48 h post-transfection, both firefly and renilla luciferase activities were measured (*A*, *upper panel*). An aliquot of cell lysates was used for immunoblot analysis (*A*, *lower panel*). HRMCs were transfected with plasmids for TGF-β1–promoter-firefly luciferase and renilla luciferase. Cells were then treated with tert-butylhydroquinone (tBHQ) for 16 h before the measurement of luciferase at 48 h post-transfection (*B*, *upper panel*). An aliquot of cell lysates was used for immunoblot analysis (*B*, *lower panel*). HRMCs were transfected with control- or Nrf2-siRNA. Then 24 h later, cells were starved before incubation with low- or high-glucose medium for an additional 24 h. Total mRNAs were extracted, and qRT-PCR was performed to measure the mRNA level of TGF-β1 (*C*). Another parallel set of cells was collected in lysis buffer for immunoblot analysis with antibodies against Nrf2, aldose reductase (AR), γGCS, NQO1, FN, and GAPDH (*D*, *upper panel*). The intensity of the bands was calculated and quantified (*D*, *lower panel*). All the experiments were repeated three times and data represent means ± SD.

Nrf2 negatively regulated TGF-β1 and FN in HRMCs. To confirm the negative effects of Nrf2 on TGF-β1, as observed in the in vivo study shown in Fig. 5*B*, regulation of the TGF-β1 promoter activity by Nrf2 was studied using luciferase reporter gene analysis. Overexpression of Nrf2 inhibited the promoter activity of TGF-β1 in a dose-dependent manner (Fig. 7*A*, *upper panel*, $*P < 0.05$). Overexpression of Nrf2 was confirmed by immunoblot analysis with an anti-HA antibody (Fig. 7*A*, *lower anti-HA panel*). Consistent with the result obtained from overexpressed Nrf2, induction of endogenous Nrf2 by tert-butylhydroquinone inhibited the promoter activity of TGF-β1 in a dose-dependent manner (Fig. 7*B*, *upper panel*, $*P < 0.05$, and *lower anti-Nrf2 panel*). Consistent with the Nrf2-mediated negative regulation of the TGF-β1 promoter, Nrf2 also negatively regulated the protein level of FN, a TGF-β1–downstream gene (Fig. 7*A* and *B*, *FN panel*). In addition, changes in TGF-β1 mRNA in response to reduced expression of Nrf2 by Nrf2-siRNA were measured in cells growing in low- and high-glucose medium. As expected, cells growing in high glucose medium had a higher level of TGF-β1 expression (Fig. 7*C*, $*P < 0.05$). Knockdown of

Nrf2 significantly enhanced the mRNA level of TGF-β1 in both conditions (Fig. 7*C*, #$P < 0.05$), again demonstrating the negative effect of Nrf2 on TGF-β1 expression. Next, another parallel set of samples was used for immunoblot analysis. High glucose induced Nrf2, aldose reductase, γGCS, and NQO1, as well as FN (Fig. 7*D*, compare *lane 1* and *3*, *$P < 0.05$). Nrf2-siRNA reduced the protein levels of Nrf2, aldose reductase, γGCS, and NQO1, while it enhanced FN in both low- and high-glucose medium (Fig. 7*D*, compare *lane 1* and *2*, and *lane 3* and *4*, #$P < 0.05$).

DISCUSSION

In the present study, a protective role of Nrf2 against diabetic nephropathy is clearly demonstrated through multiple approaches. First, human kidney tissues were used, and the results indicate that the glomeruli of human diabetic nephropathy patients were under oxidative stress, as demonstrated by oxidative DNA damage and activation of the Nrf2-mediated pathway. Second, a STZ-induced diabetes mouse model in $Nrf2^{-/-}$ mice was used to demonstrate the importance of Nrf2 in alleviating hyperglycemia-induced renal damage. $Nrf2^{-/-}$ mice had higher ROS production and suffered from greater oxidative DNA damage. This was recapitulated in HRMCs using media containing high glucose, showing an increase in ROS, which was attenuated when the cells were treated with the antioxidant supplement NAC (Fig. 6*D*). In addition, $Nrf2^{-/-}$ mice manifested severe proteinuria and glomerulosclerosis and thus suffered a greater degree of renal injury than $Nrf2^{+/+}$ mice. Consistent with our findings that Nrf2 plays an important role in alleviating renal damage caused by ROS production, Liu et al. (34) demonstrated that renal function, histology, vascular permeability, and survival were significantly worse in $Nrf2^{-/-}$ mice under ischemic conditions, which was blocked by NAC or glutathione treatment. To further verify that Nrf2 protects against ROS, a future in vivo study should be conducted using NAC or glutathione to confirm that antioxidants reduce ROS-induced damage in $Nrf2^{-/-}$ mice.

Finally, the possibility that Nrf2 negatively regulates TGF-β1 and its downstream events, such as ECM production, was explored both in mice and in cultured mesangial cells. Strikingly, the basal mRNA level of TGF-β1, FN, and collagen IV in $Nrf2^{-/-}$ mice was increased significantly compared with $Nrf2^{+/+}$ mice, indicating the negative effect of Nrf2 on the TGF-β1 pathway. This notion was further confirmed by the higher basal and induced protein levels of FN in $Nrf2^{-/-}$ mice. In HRMCs, high glucose induced ROS production and activated expression of Nrf2 and its downstream genes. Furthermore, the activation or overexpression of Nrf2 inhibited the promoter activity of TGF-β1 in a dose-dependent manner, whereas knockdown of Nrf2 by siRNA enhanced TGF-β1 transcription and FN production. This work clearly establishes a critical role of Nrf2 in protecting against diabetic nephropathy.

Because Nrf2 and NQO1 were upregulated exclusively in the kidneys of all eight diabetic nephropathy patients, it is most likely that the Nrf2-mediated antioxidant response pathway is intact in diabetic nephropathy patients. Then the question is, why did the Nrf2-mediated antioxidant response fail to protect these patients with diabetic nephropathy? We believe that activation of Nrf2 before disease development or during the early stage of diabetic nephropathy is the key for intervention to prevent ROS-induced damage and diabetic nephropathy progression. At the late stage of diabetic nephropathy, the Nrf2-mediated protective mechanism is saturated by excessive ROS, resulting in renal damage. Elucidation of the Nrf2-mediated defense system as a protective mechanism against diabetic nephropathy will help us to develop novel therapeutic interventions targeting Nrf2 to prevent or slow the progression of diabetic nephropathy.

Based on the findings from this study, we propose a model by which Nrf2 confers protection again diabetic nephropathy. Under hyperglycemic conditions, glomerular cells produce excessive amounts of ROS, which elicits many responses having both beneficial and harmful outcomes in terms of renal function. Upregulation of TGF-β1 by ROS will lead to excessive production of ECM, resulting in glomerular sclerosis/fibrosis, and ultimately loss of renal function. In addition, ROS may directly damage macromolecules, such as DNA, proteins, and lipids, which results in renal cell death and loss of function. To prevent ROS-induced damage, cells have evolved the Nrf2-mediated defense mechanism to cope with deleterious conditions. Activation of Nrf2 by stress improves renal function through at least the following two mechanisms: first is to neutralize ROS and thus reduce ROS-mediated damage, and second is to downregulate TGF-β1 and therefore alleviate ECM production. Currently, the detailed mechanism by which Nrf2 downregulates the transcription of TGF-β1 is unclear. Whether Nrf2 negatively regulates TGF-β1 by direct binding to the promoter region of TGF-β1, or by reducing ROS and ROS-induced upregulation of TGF-β1, is currently under investigation.

ACKNOWLEDGMENTS

This study was supported by ES015010 (National Institutes of Health), RSG-07-154 (American Cancer Society) (to D.D.Z.), a center grant ES006694, and NSFC 30600569 (to T.J.).

No potential conflicts of interest relevant to this article were reported.

REFERENCES

1. Ismail N, Becker B, Strzelczyk P, Ritz E. Renal disease and hypertension in non-insulin-dependent diabetes mellitus. Kidney Int 1999;55:1–28
2. Cooper ME. Pathogenesis, prevention, and treatment of diabetic nephropathy. Lancet 1998;352:213–219
3. Zheng F, Guan Y. Thiazolidinediones: a novel class of drugs for the prevention of diabetic nephropathy? Kidney Int 2007;72:1301–1303
4. Debnam ES, Unwin RJ. Hyperglycemia and intestinal and renal glucose transport: implications for diabetic renal injury. Kidney Int 1996;50:1101–1109
5. Jeong SO, Oh GS, Ha HY, Soon Koo B, Sung Kim H, Kim YC, Kim EC, Lee KM, Chung HT, Pae HO. Dimethoxycurcumin, a synthetic curcumin analogue, induces Heme oxygenase-1 expression through Nrf2 activation in RAW264.7 macrophages. J Clin Biochem Nutr 2009;44:79–84
6. Fridlyand LE, Philipson LH. Oxidative reactive species in cell injury: mechanisms in diabetes mellitus and therapeutic approaches. Ann N Y Acad Sci 2005;1066:136–151
7. Kiritoshi S, Nishikawa T, Sonoda K, Kukidome D, Senokuchi T, Matsuo T, Matsumura T, Tokunaga H, Brownlee M, Araki E. Reactive oxygen species from mitochondria induce cyclooxygenase-2 gene expression in human mesangial cells: potential role in diabetic nephropathy. Diabetes 2003;52:2570–2577
8. Lee EA, Seo JY, Jiang Z, Yu MR, Kwon MK, Ha H, Lee HB. Reactive oxygen species mediate high glucose-induced plasminogen activator inhibitor-1 up-regulation in mesangial cells and in diabetic kidney. Kidney Int 2005;67:1762–1771
9. Thallas-Bonke V, Thorpe SR, Coughlan MT, Fukami K, Yap FY, Sourris KC, Penfold SA, Bach LA, Cooper ME, Forbes JM. Inhibition of NADPH oxidase prevents advanced glycation end product-mediated damage in diabetic nephropathy through a protein kinase C-alpha-dependent pathway. Diabetes 2008;57:460–469

10. Koya D, Hayashi K, Kitada M, Kashiwagi A, Kikkawa R, Haneda M. Effects of antioxidants in diabetes-induced oxidative stress in the glomeruli of diabetic rats. J Am Soc Nephrol 2003;14:S250–S253
11. Itoh K, Ishii T, Wakabayashi N, Yamamoto M. Regulatory mechanisms of cellular response to oxidative stress. Free Radic Res 1999;31:319–324
12. Kensler TW, Wakabayashi N, Biswal S. Cell survival responses to environmental stresses via the Keap1-Nrf2-ARE pathway. Annu Rev Pharmacol Toxicol 2007;47:89–116
13. Zhang DD. Mechanistic studies of the Nrf2-Keap1 signaling pathway. Drug Metab Rev 2006;38:769–789
14. Chan K, Han XD, Kan YW. An important function of Nrf2 in combating oxidative stress: detoxification of acetaminophen. Proc Natl Acad Sci U S A 2001;98:4611–4616
15. Cho HY, Reddy SP, Kleeberger SR. Nrf2 defends the lung from oxidative stress. Antioxid Redox Signal 2006;8:76–87
16. Xue M, Qian Q, Adaikalakoteswari A, Rabbani N, Babaei-Jadidi R, Thornalley PJ. Activation of NF-E2-related factor-2 reverses biochemical dysfunction of endothelial cells induced by hyperglycemia linked to vascular disease. Diabetes 2008;57:2809–2817
17. He X, Kan H, Cai L, Ma Q. Nrf2 is critical in defense against high glucose-induced oxidative damage in cardiomyocytes. J Mol Cell Cardiol 2009;46:47–58
18. Yoh K, Hirayama A, Ishizaki K, Yamada A, Takeuchi M, Yamagishi S, Morito N, Nakano T, Ojima M, Shimohata H, Itoh K, Takahashi S, Yamamoto M. Hyperglycemia induces oxidative and nitrosative stress and increases renal functional impairment in Nrf2-deficient mice. Genes Cells 2008;13:1159–1170
19. Yamamoto T, Nakamura T, Noble NA, Ruoslahti E, Border WA. Expression of transforming growth factor beta is elevated in human and experimental diabetic nephropathy. Proc Natl Acad Sci U S A 1993;90:1814–1818
20. Yokoyama H, Deckert T. Central role of TGF-beta in the pathogenesis of diabetic nephropathy and macrovascular complications: a hypothesis. Diabet Med 1996;13:313–320
21. Yamamoto T, Noble NA, Cohen AH, Nast CC, Hishida A, Gold LI, Border WA. Expression of transforming growth factor-beta isoforms in human glomerular diseases. Kidney Int 1996;49:461–469
22. Yamamoto T, Noble NA, Miller DE, Gold LI, Hishida A, Nagase M, Cohen AH, Border WA. Increased levels of transforming growth factor-beta in HIV-associated nephropathy. Kidney Int 1999;55:579–592
23. Yamamoto T, Watanabe T, Ikegaya N, Fujigaki Y, Matsui K, Masaoka H, Nagase M, Hishida A. Expression of types I, II, and III TGF-beta receptors in human glomerulonephritis. J Am Soc Nephrol 1998;9:2253–2261
24. Gupta S, Clarkson MR, Duggan J, Brady HR. Connective tissue growth factor: potential role in glomerulosclerosis and tubulointerstitial fibrosis. Kidney Int 2000;58:1389–1399
25. Border WA, Ruoslahti E. Transforming growth factor-beta 1 induces extracellular matrix formation in glomerulonephritis. Cell Differ Dev 1990;32:425–431
26. Bakin AV, Stourman NV, Sekhar KR, Rinehart C, Yan X, Meredith MJ, Arteaga CL, Freeman ML. Smad3-ATF3 signaling mediates TGF-beta suppression of genes encoding Phase II detoxifying proteins. Free Radic Biol Med 2005;38:375–387
27. Choi HK, Pokharel YR, Lim SC, Han HK, Ryu CS, Kim SK, Kwak MK, Kang KW. Inhibition of liver fibrosis by solubilized coenzyme Q10: Role of Nrf2 activation in inhibiting transforming growth factor-beta1 expression. Toxicol Appl Pharmacol 2009;240:377–384
28. Chan K, Lu R, Chang JC, Kan YW. NRF2, a member of the NFE2 family of transcription factors, is not essential for murine erythropoiesis, growth, and development. Proc Natl Acad Sci U S A 1996;93:13943–13948
29. Taneda S, Pippin JW, Sage EH, Hudkins KL, Takeuchi Y, Couser WG, Alpers CE. Amelioration of diabetic nephropathy in SPARC-null mice. J Am Soc Nephrol 2003;14:968–980
30. Rosen P, Nawroth PP, King G, Moller W, Tritschler HJ, Packer L. The role of oxidative stress in the onset and progression of diabetes and its complications: a summary of a Congress Series sponsored by UNESCO-MCBN, the American Diabetes Association and the German Diabetes Society. Diabetes Metab Res Rev 2001;17:189–212
31. Wei XF, Zhou QG, Hou FF, Liu BY, Liang M. Advanced oxidation protein products induce mesangial cell perturbation through PKC-dependent activation of NADPH oxidase. Am J Physiol Renal Physiol 2009;296:F427–F437
32. Roestenberg P, van Nieuwenhoven FA, Joles JA, Trischberger C, Martens PP, Oliver N, Aten J, Höppener JW, Goldschmeding R. Temporal expression profile and distribution pattern indicate a role of connective tissue growth factor (CTGF/CCN-2) in diabetic nephropathy in mice. Am J Physiol Renal Physiol 2006;290:F1344–F1354
33. Jiang T, Che Q, Lin Y, Li H, Zhang N. Aldose reductase regulates TGF-beta1-induced production of fibronectin and type IV collagen in cultured rat mesangial cells. Nephrology (Carlton) 2006;11:105–112
34. Liu M, Grigoryev DN, Crow MT, Haas M, Yamamoto M, Reddy SP, Rabb H. Transcription factor Nrf2 is protective during ischemic and nephrotoxic acute kidney injury in mice. Kidney Int 2009;76:277–285